JOINT EUROPEAN TORUS

JET–P(92)99

R.C. Wolf, J. O'Rourke, A.W. Edwards, M von Hellermann
and JET Team

Comparison of Poloidal Field Measurements on JET

Comparison of Poloidal Field Measurements on JET

R.C. Wolf, J. O'Rourke, A.W. Edwards, M von Hellermann
and JET Team*

JET-Joint Undertaking, Culham Science Centre, OX14 3DB, Abingdon, UK

** See Annex*

Preprint of Paper to be submitted for publication in
Nuclear Fusion (Letters)

COMPARISON OF POLOIDAL FIELD MEASUREMENTS ON JET

R C Wolf, J O'Rourke, A W Edwards, M von Hellermann

JET Joint Undertaking, Abingdon, OX14 3EA, G.B.

ABSTRACT

Simultaneous measurements of the poloidal magnetic field distribution in JET by means of the Faraday and motional Stark effects are reported. The experiments were designed to minimize errors resulting from non-circular flux surface geometry and limited spatial resolution. Both techniques show that full reconnection of the flux inside the q = 1 surface does not occur during a sawtooth collapse.

1. INTRODUCTION

The central safety factor in sawtoothing tokamak discharges has been measured using a variety of diagnostic techniques /1/, with seemingly contradictory results /2-13/. The technique which is closest to being a "standard" diagnostic is that of far-infrared polarimetry (Faraday rotation) /14/. Low values of the axial safety factor in sawtoothing discharges, $q_o \sim 0.75$, have been inferred from this measurement /3,6/. A number of other techniques /4,7,10,11/ indicate on the contrary that q_o is very close to 1 throughout the sawtooth cycle. This raises the possibility that the interpretation of the Faraday effect measurements is in error. The issue has serious implications for the understanding of the sawtooth instability and the magnetic reconnection process which accompanies it /15,16/.

Until now, no direct confrontation of the Faraday effect measurements with another diagnostic technique has been made. One difficulty in carrying out such a comparison is the effort of mounting at least two complex diagnostics of the poloidal field on a given machine. Another stems from the partial incompatibility of the plasma parameters required for different measurements.

A second technique which has been very successfully devoloped in recent years makes use of the motional Stark effect (MSE) /17,9,13/. In this paper we present the first direct comparison of the poloidal field measurements obtained using the Faraday and motional Stark effects.

The measurements are made by an 8-channel DCN (195 μm) far-infrared polarimeter /18/ and by a 4-channel visible beam-emission spectrometer, which measures both the magnitude of the Stark splitting and the polarization of the multiplet components.

In the following section we present some details on the experimental set-up necessitated by the nature of the diagnostics. In section 3 we compare the evolution of the q-profile deduced by these two techniques. Conclusions and a brief discussion of the implications of the results are found in section 4.

2. EXPERIMENTAL ARRANGEMENT AND CONSISTENCY CHECKS

An important source of error in deducing the safety factor profile from a measurement of the poloidal field is the uncertainty in the geometry of the magnetic flux surfaces, especially their elongation. This is true of any poloidal field measurement and arises from the fact that the safety factor is a flux surface averaged quantity. Knowledge of the magnetic geometry is particularly important in the case of Faraday rotation since it is also needed to Abel-invert the line-integrated measurements to obtain local quantities. For a given elongation of the plasma boundary, κ_b, the elongation of the internal flux surfaces is in the range $1 < \kappa < \kappa_b$. Therefore in discharges with $\kappa_b = 1$, ie., circular discharges, the geometric sources of error are minimized. In the experiments reported here, circular magnetic equilibria were used. This has been verified by the equilibrium identification code IDENTD (which incorporates both magnetic and polarimetric measurements) and by tomographic inversion of the soft X-ray emmissivity. Both determinations give $\kappa = 1$ within 3%.

The discharges have moderate toroidal field ($B_T = 2.8T$) to avoid birefringence and to produce a reasonably large q = 1 surface. The electron density is also moderate ($2.5 \bullet 10^{19} m^{-3}$) to obtain good beam penetration without having inordinately small Faraday rotation angles. The plasma current is scanned in the range 1 - 3 MA.

An important source of error in non-local measurements like that of Faraday rotation lies in the number of probing chords. To alleviate this problem, major radius sweeps of the plasma column were introduced. This increases the effective spatial resolution of the diagnostic, since successive time points probe different relative positions in the plasma. In the case of local measurements like that of the motional Stark effect,

radial sweeps are also useful for eliminating systematic errors which result in offsets in the measured angle of inclination of the magnetic field.

An independent check of the q profile determination is provided by the sawtoothing behaviour diagnosed by the SXR camera. For the discharges in this series, the value of q_o (determined from Faraday rotation) at which sawtoothing is observed to begin is 0.97 ± 0.06. Comparison of the size of the SXR inversion radius with that of the q = 1 surface shows agreement within $\pm$ 5 cm., except at the highest values of q_a (~ 8), when q_o is very close to 1 and a small change in q leads to a very large change in the radius of the q = 1 surface.

3. COMPARISON OF MOTIONAL STARK AND FARADAY EFFECT MEASUREMENTS

Figure 1 shows the poloidal field distribution determined by Abel inversion of the Faraday rotation data. Also shown are the local measurements obtained by the MSE diagnostic and their statistical errors. The pitch of the magnetic field deduced from the MSE measurements is subject to a calibration error of about 1°. For a toroidal field of 2.8 T this corresponds to an error of 0.05 T. Thus the absolute measurements of the Faraday and MSE diagnostics are consistent, but the MSE measurements do not reduce the error in the inferred magnetic field within the q = 1 surface (2.6 m < R < 3.5 m.).

A more stringent constraint is provided by relative changes in the data arising from their time evolution or from radial displacements. Here only statistical (signal-to-noise) errors in the MSE data need to be considered. The systematic error introduced by offsets is irrelevant since we are looking at the changes in the poloidal field.

Figure 2 shows the evolution of the Faraday and MSE data during the current penetration phase. One of the radii shown (3.43 m.) is some 5 cm. outside the SXR inversion radius at the first sawtooth; the second (3.24 m.) is well inside it. Both diagnostics indicate a substantial rise in the poloidal field within the q = 1 surface following the onset of sawtoothing, implying that q_o reaches a value below 1.

Figure 3 shows the time evolution of the central chord of the polarimeter as the plasma is displaced in and out across the line of sight. Note that the periodic modulation arising from sawtoothing have been subtracted to highlight the effect of the radial sweep. Also shown are the calculated values of the Faraday angle under the assumption that (1) the q-profile is flat within the SXR inversion radius or that (2) the q-profile is hollow

within this radius, reaching a value of 0.75 at the axis (Figure 9). The latter assumption clearly gives a better fit to the data. Figure 4 compares the effect of the same radial sweep on the MSE measurement with simulations. Since this is a local measurement, it only depends on the local value of the safety factor and shear:

$$\Delta\left(\frac{B_p}{B_T}\right) = \frac{\Delta r}{Rq}\left[1 - \frac{r}{q}\frac{dq}{dr}\right]$$

The simulations are made assuming a constant value of q at the measurement position ($dq/dr = 0$). Thus the inferred value of q represents an upper bound if the q profile is assumed to be monotonically increasing with radius. As with the variation of the Faraday angle, the change in the observed pitch angle is consistent with a value of q well below 1 inside the q = 1 surface.

In order to understand the sawtooth process, it is important to quantify how much reconnection of the poloidal flux occurs at a collapse. Previous analysis of the Faraday data /19/ suggests that the change in q_o at a collapse is correlated with the length of the preceding sawtooth period (Figure 5). For sawtooth periods below about 300 msec., the MSE diagnostic does not have sufficient resolution to address this question. However it can detect the changes which occur in sawteeth having longer periods, for example ICRF-produced "Monster" sawteeth (figure 6). The change in q_o which is inferred from such data is also shown in figure 5, and demonstrates the consistency of the 2 diagnostics.

4. CONCLUSIONS

The most important sources of error in the determination of the q-profile in JET are (1) the complicated geometry and (2) the non-local nature of the Faraday rotation diagnostic. and (3) systematic offsets in the pitch angles measured using motional Stark effect polarimetry. The first of these problems has been adressed by experiments in strictly circular discharges; the second and third, by radial sweeps of the plasma.

Under these optimized conditions, both diagnostics lead to similar inferences regarding the safety factor profile in tokamaks. The consistent result which emerges is that the safety factor is well below unity throughout the sawtooth cycle. The actual value depends on experimental conditions, but values in the range 0.7 - 0.85 are typical. Partial reconnection of the poloidal flux does occur. The mechanism

which halts the reconnection process once it has begun is not understood and poses a major challenge for sawtooth theory.

This publication forms part of a doctoral thesis by one of the authors (RCW) at the University of Dusseldorf, FRG.

REFERENCES

/1/ H Soltwisch
Plasma Physics and Controlled Fusion 34(1992)1669.

/2/ M J Forrest, P G Carolan and N J Peacock
Nature 271(1978)718.

/3/ H Soltwisch, W Stodiek, J Manickamn J Schluter
Plasma Physics and Controlled Nuclear Fusion Research 1986,
Vol. I, p. 263, IAEA, Vienna.

/4/ K McCormick, F X Soldner, D Eckhartt et al.
Phys. Rev. Lett. 58(1987)491.

/5/ W P West, D M Thomas, J S de Grassie and S B Zheng
Phys. Rev. Lett. 58(1987)2758.

/6/ J O'Rourke, J Blum, J G Cordey et al.
15th Euro. Conf. on Contr. Fusion and Plasma Heating, Dubrovnik, 1988.
Vol 12B, part I, p. 155, EPS, Geneva.

/7/ D Wroblewski, L K Huang, H W Moos and P E Phillips
Phys. Rev. Lett. 61(1988)1724.

/8/ R A Moyer, J A Goetz, R N Dexter, and S C Prager
Physics Fluids B 1(1989)2139.

/9/ F M Levinton, R J Fonck, G M Gammel et al.
Phys. Rev. Lett. 63(1989)2060.

/10/ H Weisen, et al..
Phys. Rev. Lett. 62(1989)434.

/11/ L K Huang, M Finkenthal, D Wroblewski et al.
Physics Fluids B 2(1990)809.

/12/ P Descamps, G van Wassenhove, R Koch et al.
Phys. Lett 143A(1990)311.

/13/ D Wroblewski, L L Lao
Physics Fluids B 3(1991)2877.

/14/ H Soltwisch
Basic and Advanced Diagnostic Techniques, Varenna, 1986

Vol. 2, p343, CEC, Brussels.

/15/ B B Kadomtsev
Fiz. Plazmy 1(1975)750

/16/ J Wesson
Plasma Physics and Controlled Fusion 28(1986)243.

/17/ A Boileau, M von Hellermann, W Mandl, et al.
J. Phys. B: At. Mol. Opt. Phys. 22(1989)L145.

/18/ G Braithwaite, N Gottardi, G Magyar et al.
Rev. Scient. Instrum. 60(1989)2825.

/19/ J O'Rourke
Plasma Physics and Controlled Fusion, 33(1991)289.

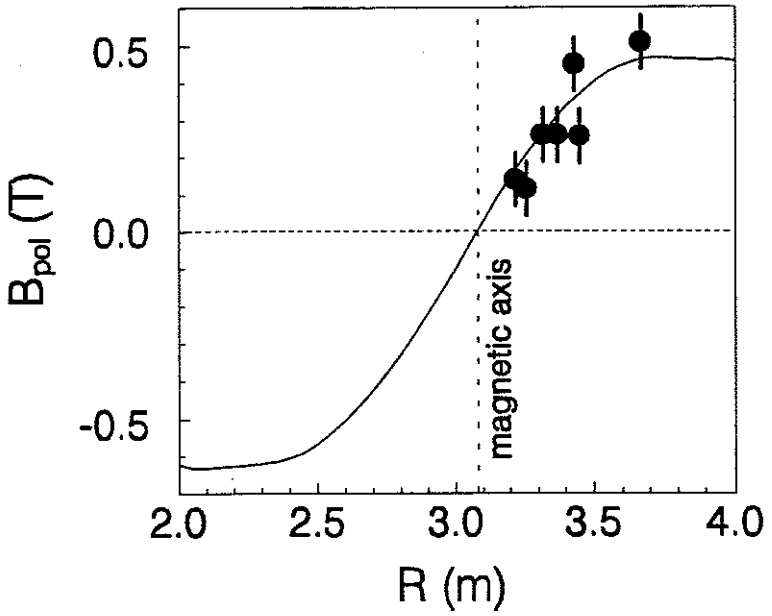

Figure 1. Poloidal field distribution determined from Faraday rotation (solid line) and MSE measurements (circles). Two identical discharges in which the MSE measurement positions were scanned are overlaid.

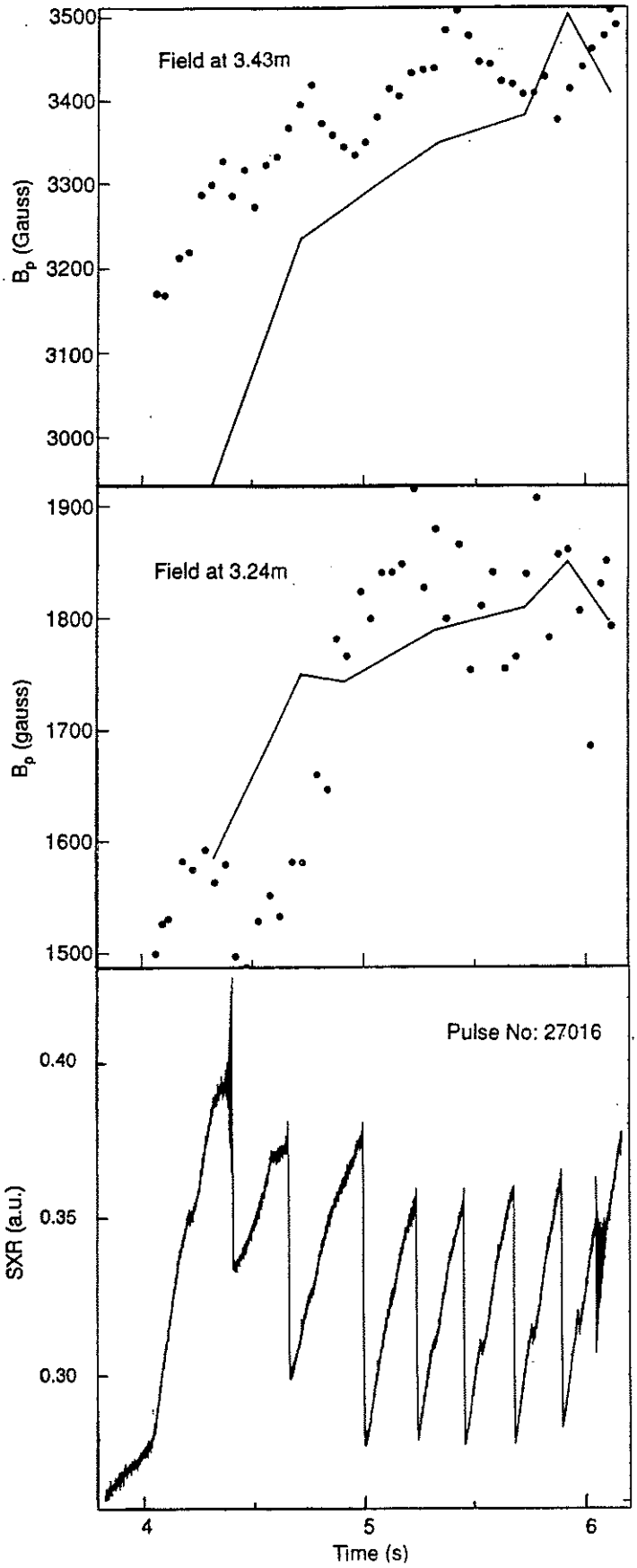

Figure 2. Time evolution of the poloidal field during the current penetration phase in pulse 27016. Faraday rotation (solid lines), MSE (circles). Also shown is the evolution of the central safety factor inferred from Faraday rotation and a central SXR signal.

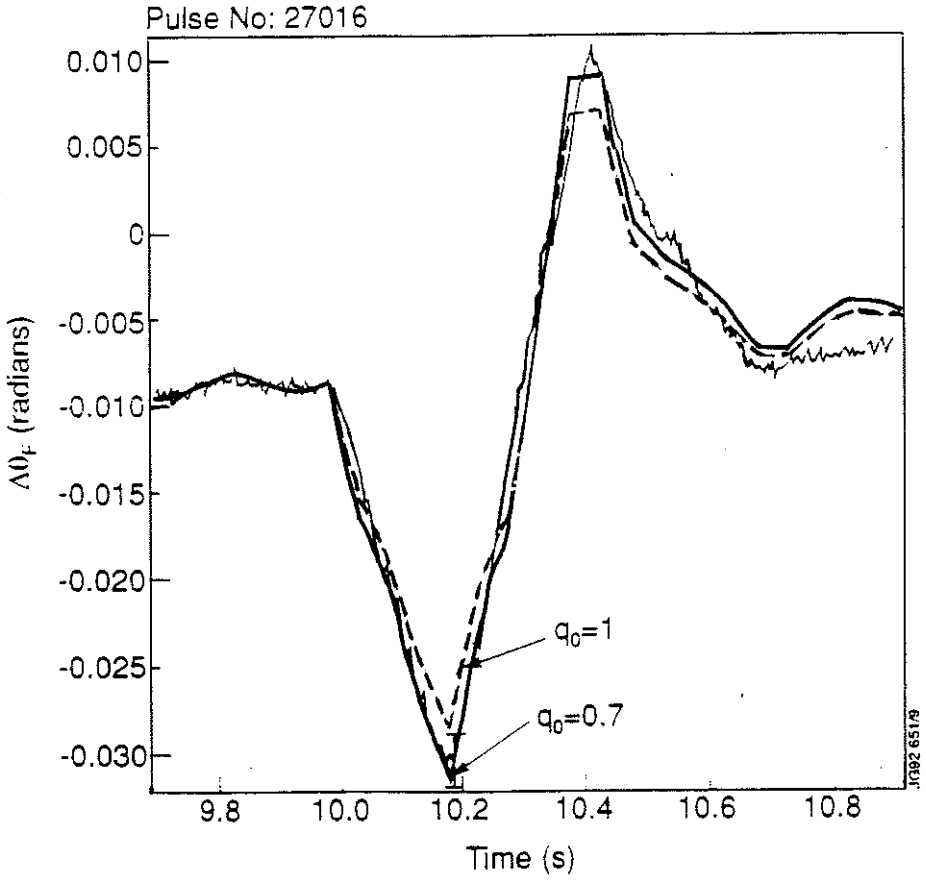

Figure 3. Change in Faraday angle on a central chord (R=3.02 m.) during a radial plasma sweep. Also shown are calculations assuming q_o = 1 (dashed line) and q_o = 0.75 (solid line).

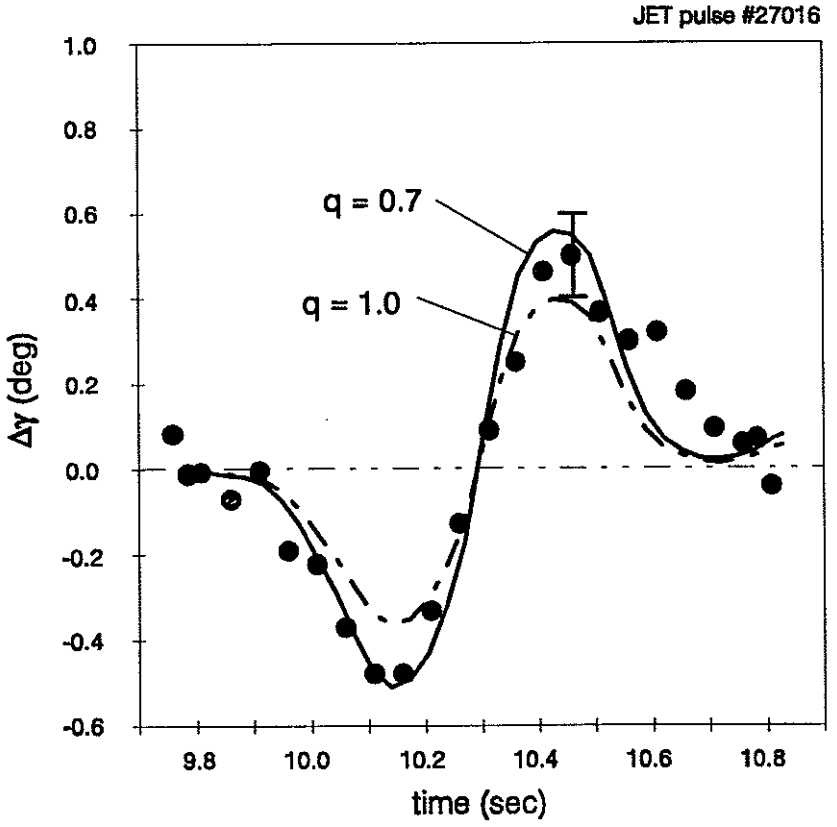

Figure 4. Change in the pitch of the magnetic field during a radial plasma sweep, inferred from the MSE measurements. Also shown are calculations assuming vanishing shear and q = 0.7 (solid line) and 1.0 (dashed line).

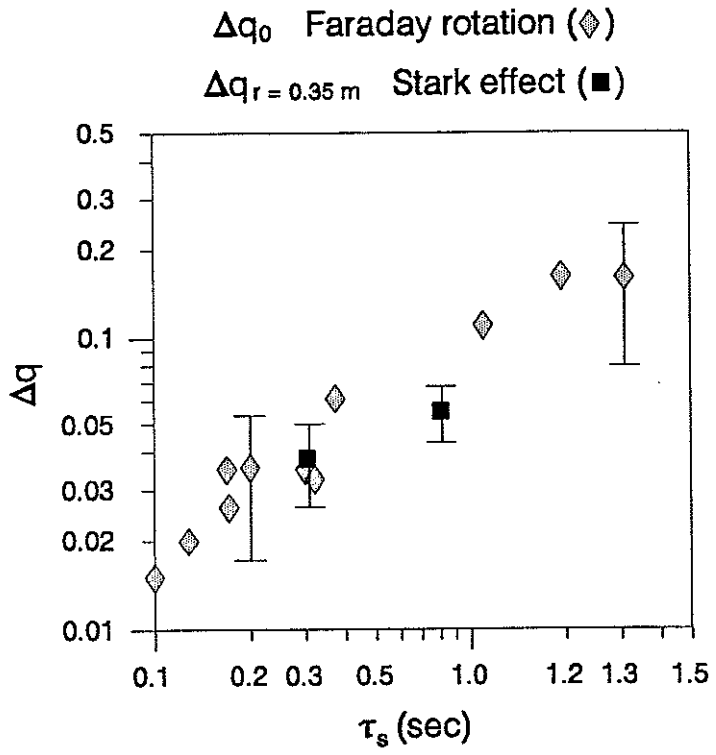

Figure 5. Change in q_o at a sawtooth collapse versus preceding sawtooth period. Faraday rotation (diamonds), MSE (squares).

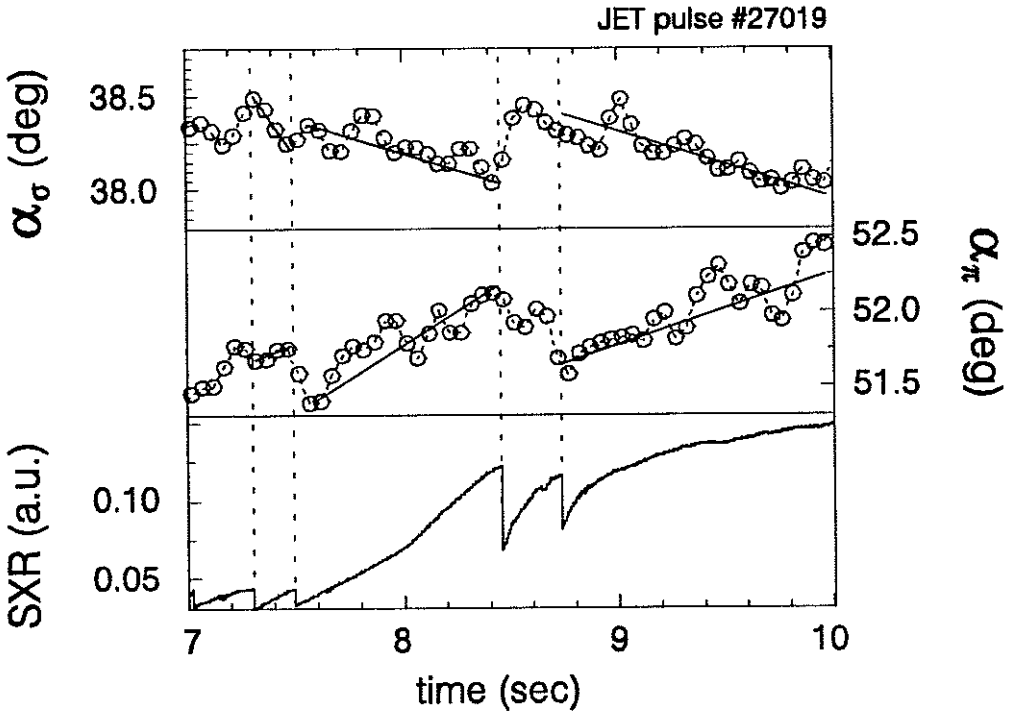

Figure 6. Evolution of the σ and π polarizations during a "Monster" sawtooth. Also shown is a central SXR signal.

Appendix I

THE JET TEAM

JET Joint Undertaking, Abingdon, Oxon, OX14 3EA, U.K.

J.M. Adams[1], B. Alper, H. Altmann, A. Andersen[14], P. Andrew, S.Ali-Arshad, W. Bailey, B. Balet, P. Barabaschi, Y. Baranov, P. Barker, R. Barnsley[2], M. Baronian, D.V. Bartlett, A.C. Bell, G. Benali, P. Bertoldi, E. Bertolini, V. Bhatnagar, A.J. Bickley, D. Bond, T. Bonicelli, S.J. Booth, G. Bosia, M. Botman, D. Boucher, P. Boucquey, M. Brandon, P. Breger, H. Brelen, W.J. Brewerton, H. Brinkschulte, T. Brown, M. Brusati, T. Budd, M. Bures, P. Burton, T. Businaro, P. Butcher, H. Buttgereit, C. Caldwell-Nichols, D.J. Campbell, D. Campling, P. Card, G. Celentano, C.D. Challis, A.V.Chankin[23], A. Cherubini, D. Chiron, J. Christiansen, P. Chuilon, R. Claesen, S. Clement, E. Clipsham, J.P. Coad, I.H. Coffey[24], A. Colton, M. Comiskey[4], S. Conroy, M. Cooke, S. Cooper, J.G. Cordey, W. Core, G. Corrigan, S. Corti, A.E. Costley, G. Cottrell, M. Cox[7], P. Crawley, O. Da Costa, N. Davies, S.J. Davies[7], H. de Blank, H. de Esch, L. de Kock, E. Deksnis, N. Deliyanakus, G.B. Denne-Hinnov, G. Deschamps, W.J. Dickson[19], K.J. Dietz, A. Dines, S.L. Dmitrenko, M. Dmitrieva[25], J. Dobbing, N. Dolgetta, S.E. Dorling, P.G. Doyle, D.F. Düchs, H. Duquenoy, A. Edwards, J. Ehrenberg, A. Ekedahl, T. Elevant[11], S.K. Erents[7], L.G. Eriksson, H. Fajemirokun[12], H. Falter, J. Freiling[15], C. Froger, P. Froissard, K. Fullard, M. Gadeberg, A. Galetsas, L. Galbiati, D. Gambier, M. Garribba, P. Gaze, R. Giannella, A. Gibson, R.D. Gill, A. Girard, A. Gondhalekar, D. Goodall[7], C. Gormezano, N.A. Gottardi, C. Gowers, B.J. Green, R. Haange, A. Haigh, C.J. Hancock, P.J. Harbour, N.C. Hawkes[7], N.P. Hawkes[1], P. Haynes[7], J.L. Hemmerich, T. Hender[7], J. Hoekzema, L. Horton, J. How, P.J. Howarth[5], M. Huart, T.P. Hughes[4], M. Huguet, F. Hurd, K. Ida[18], B. Ingram, M. Irving, J. Jacquinot, H. Jaeckel, J.F. Jaeger, G. Janeschitz, Z. Jankowicz[22], O.N. Jarvis, F. Jensen, E.M. Jones, L.P.D.F. Jones, T.T.C. Jones, J-F. Junger, F. Junique, A. Kaye, B.E. Keen, M. Keilhacker, W. Kerner, N.J. Kidd, R. Konig, A. Konstantellos, P. Kupschus, R. Lässer, J.R. Last, B. Laundy, L. Lauro-Taroni, K. Lawson[7], M. Lennholm, J.Lingertat[13], R.N. Litunovski, A. Loarte, R. Lobel, P. Lomas, M. Loughlin, C. Lowry, A.C. Maas[15], B. Macklin, C.F. Maggi[16], G. Magyar, V. Marchese, F. Marcus, J. Mart, D. Martin, E. Martin, R. Martin-Solis[8], P. Massmann, G. Matthews, H. McBryan, G. McCracken[7], P. Meriguet, P. Miele, S.F. Mills, P. Millward, E. Minardi[16], R. Mohanti[17], P.L. Mondino, A. Montvai[3], P. Morgan, H. Morsi, G. Murphy, F. Nave[27], S. Neudatchin[23], G. Newbert, M. Newman, P. Nielsen, P. Noll, W. Obert, D. O'Brien, J. O'Rourke, R. Ostrom, M. Ottaviani, S. Papastergiou, D. Pasini, B. Patel, A. Peacock, N. Peacock[7], R.J.M. Pearce, D. Pearson[12], J.F. Peng[26], R. Pepe de Silva, G. Perinic, C. Perry, M.A. Pick, J. Plancoulaine, J-P. Poffé, R. Pohlchen, F. Porcelli, L. Porte[19], R. Prentice, S. Puppin, S. Putvinskii[23], G. Radford[9], T. Raimondi, M.C. Ramos de Andrade, M. Rapisarda[29], P-H. Rebut, R. Reichle, S. Richards, E. Righi, F. Rimini, A. Rolfe, R.T. Ross, L. Rossi, R. Russ, H.C. Sack, G. Sadler, G. Saibene, J.L. Salanave, G. Sanazzaro, A. Santagiustina, R. Sartori, C. Sborchia, P. Schild, M. Schmid, G. Schmidt[6], H. Schroepf, B. Schunke, S.M. Scott, A. Sibley, R. Simonini, A.C.C. Sips, P. Smeulders, R. Smith, M. Stamp, P. Stangeby[20], D.F. Start, C.A. Steed, D. Stork, P.E. Stott, P. Stubberfield, D. Summers, H. Summers[19], L. Svensson, J.A. Tagle[21], A. Tanga, A. Taroni, C. Terella, A. Tesini, P.R. Thomas, E. Thompson, K. Thomsen, P. Trevalion, B. Tubbing, F. Tibone, H. van der Beken, G. Vlases, M. von Hellermann, T. Wade, C. Walker, D. Ward, M.L. Watkins, M.J. Watson, S. Weber[10], J. Wesson, T.J. Wijnands, J. Wilks, D. Wilson, T. Winkel, R. Wolf, D. Wong, C. Woodward, M. Wykes, I.D. Young, L. Zannelli, A. Zolfaghari[28], G. Zullo, W. Zwingmann.

PERMANENT ADDRESSES

1. UKAEA, Harwell, Didcot, Oxon, UK.
2. University of Leicester, Leicester, UK.
3. Central Research Institute for Physics, Budapest, Hungary.
4. University of Essex, Colchester, UK.
5. University of Birmingham, Birmingham, UK.
6. Princeton Plasma Physics Laboratory, New Jersey, USA.
7. UKAEA Culham Laboratory, Abingdon, Oxon, UK.
8. Universidad Complutense de Madrid, Spain.
9. Institute of Mathematics, University of Oxford, UK.
10. Freien Universität, Berlin, F.R.G.
11. Royal Institute of Technology, Stockholm, Sweden.
12. Imperial College, University of London, UK.
13. Max Planck Institut für Plasmaphysik, Garching, FRG.
14. Risø National Laboratory, Denmark.
15. FOM Instituut voor Plasmafysica, Nieuwegein, The Netherlands.
16. Dipartimento di Fisica, University of Milan, Milano, Italy.
17. North Carolina State University, Raleigh, NC, USA
18. National Institute for Fusion Science, Nagoya, Japan.
19. University of Strathclyde, 107 Rottenrow, Glasgow, UK.
20. Institute for Aerospace Studies, University of Toronto, Ontario, Canada.
21. CIEMAT, Madrid, Spain.
22. Institute for Nuclear Studies, Otwock-Swierk, Poland.
23. Kurchatov Institute of Atomic Energy, Moscow, USSR
24. Queens University, Belfast, UK.
25. Keldysh Institute of Applied Mathematics, Moscow, USSR.
26. Institute of Plasma Physics, Academica Sinica, Hefei, P. R. China.
27. LNETI, Savacem, Portugal.
28. Plasma Fusion Center, M.I.T., Boston, USA.
29. ENEA, Frascati, Italy.

At 1st July, 1992